Magma replenishment, and the significance of poikilitic textures, in the Lower Main Zone of the western Bushveld Complex, South Africa

ANDREW A. MITCHELL

Department of Geology, University of Durban-Westville, Private Bag X54001, Durban, 4000, South Africa

HUGH V. EALES

Department of Geology, Rhodes University, Grahamstown 6140, South Africa

AND

F. JOHAN KRUGER

Hugh Allsopp Laboratory, Bernard Price Institute for Geophysical Research, Private Bag 3, Wits 2050, South Africa

ABSTRACT

Petrographic and compositional variations in the Lower Main Zone (LMZ) of the western Bushveld Complex indicate changing regimes of magma replenishment. The lowermost unit of the LMZ, designated N-I, is an enigmatic sequence of leuconoritic cumulates, characterized primarily by up-sequence increases in both orthopyroxene Mg# and whole-rock Sr isotope initial ratio. The Sr isotope profile of N-I is ascribed to injection and progressive integration of small influxes of fresh magma with high (Main Zone-type) Sr isotope initial ratios. The basal Fe-enrichment in N-I, on the other hand, is ascribed to a separate, later mechanism involving the downward migration of late-stage Fe-rich liquids. The overlying two units, N-II and G-I, delineated chiefly in terms of basal Mg-enrichment of orthopyroxene, are ascribed to injections of fresh magma into the chamber. Poikilitic orthopyroxene grains in the basal parts of both N-II and G-I suggest entrainment and partial resorption of plagioclase grains from the semi-crystalline resident material into which the fresh magma was intruded.

Introduction

THE accumulation of trace element, isotopic and mineral chemical data for the Main Zone of the Bushveld Complex in recent years (Mitchell, 1990; Kruger, 1994; Mitchell, 1996) has created new perspectives on this part of the Bushveld succession. Chemical and petrographic reversals at the Pyroxenite Marker, some 2000 to 2500 m above the base of the Main Zone (MZ), are well documented (von Gruenewaldt, 1973; Molyneux, 1974; Cawthorn *et al.*, 1991). On this basis, Mitchell (1990) subdivided the MZ of the western Bushveld into the Lower Main Zone (LMZ), constituting the sequence below the Pyroxenite

Marker, and the Upper Main Zone (UMZ) above the Pyroxenite Marker.

Below the Pyroxenite Marker, several lesser chemical inflections have been identified, especially in the composition of low-Ca pyroxene, and consequently the LMZ has itself been subdivided into a series of units (Mitchell, 1990; 1996). Of these, the lowermost two (N-I and N-II) are leuconoritic, the remainder being essentially gabbronoritic.

At the base of the Merensky Reef, which is at a variable distance of between 30 and 130 m below the base of the LMZ in the western Bushveld, there is an abrupt increase in the Sr isotope initial ratio (Kruger and Marsh, 1982), and the ratio

continues to increase through the upper part of the UCZ and into unit N-I of the LMZ. Particularly high initial ratios, typical of those commonly associated with the LMZ (Hamilton, 1977; Sharpe, 1985; Kruger, 1994) are found at the bases of units N-II and G-I. The lowermost units of the LMZ (N-I, N-II and G-I) are the focus of this study. They are important in that they represent the culmination of a transition from magmas with the isotopic signatures of the Upper Critical Zone (UCZ) to magmas with LMZ

isotopic signatures. It is the purpose of this work to investigate the lowermost three units of the LMZ (N-I, N-II and G-I), using whole-rock chemistry and mineral chemistry in conjunction with petrography, and to relate them to changing regimes of magma replenishment.

Outcrop of the MZ in the western Bushveld is extremely limited, and detailed stratigraphic and petrological data are sourced almost exclusively from exploration borehole cores. This study is based substantially on borehole SK2, drilled
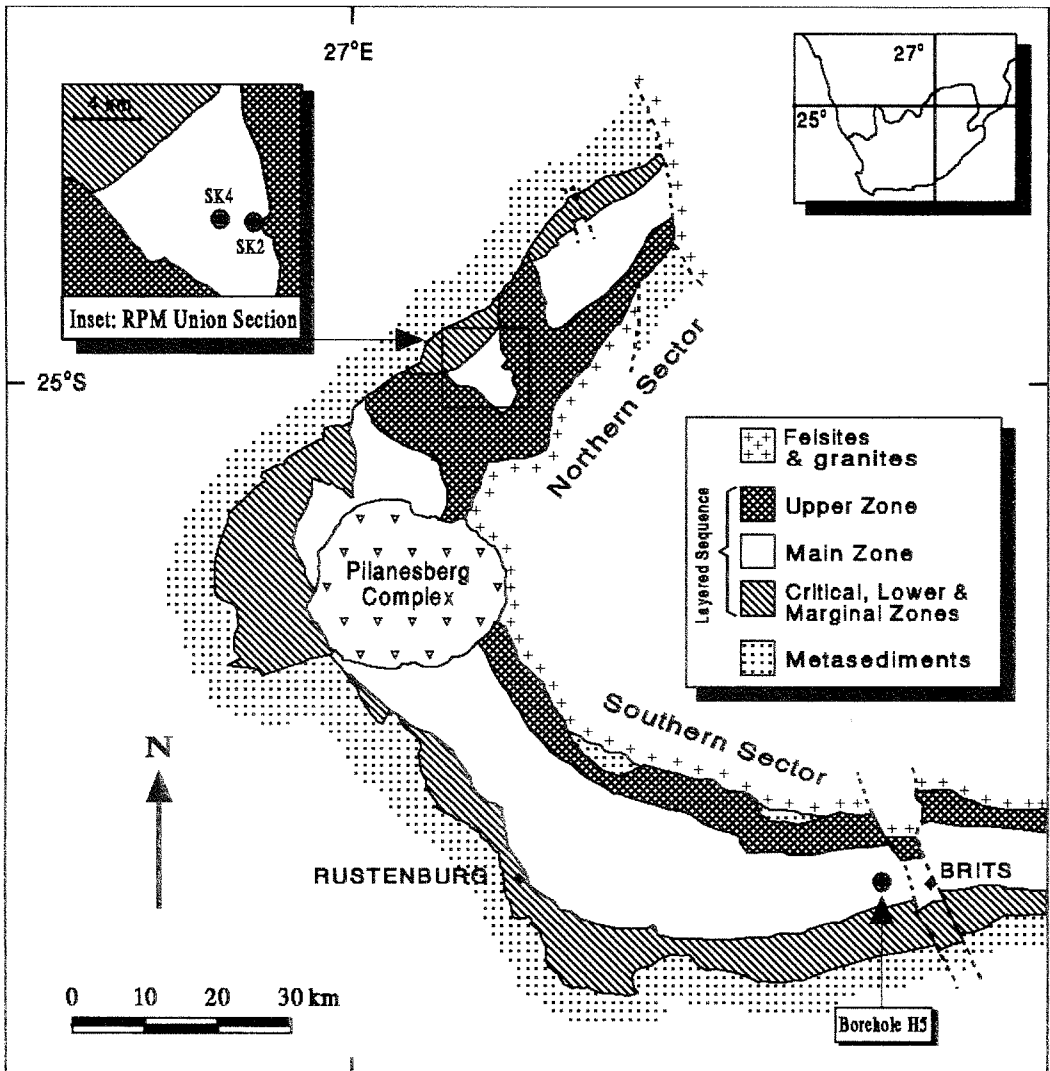

FIG. 1. Sketch map of the western Bushveld Complex, showing the position of borehole SK2, as well as boreholes SK4 and H5.

within the mining lease area of Rustenburg Platinum Mines (RPM) Union Section, in the northern sector of the western Bushveld Complex. Reference is also made to borehole SK4, which is up-dip from SK2 at RPM Union Section, and comparisons are drawn between the Union Section data and data from borehole H5, which was drilled near Brits, in the southern sector of the western Bushveld (Figs. 1 and 2). The northern sector (represented in this study by the SK2 succession) constitutes the proximal facies of the western Bushveld (Eales *et al.*, 1988, 1994; Maier and Eales, 1994a; Scoon and Teigler, 1994), being closest to the postulated magmatic feeder system. The southern sector, by contrast, constitutes the distal facies. Unless otherwise indicated, stratigraphic and petrographic descriptions given in the text refer to the succession in borehole SK2.

Stratigraphy and petrography

Unit N-I

Unit N-I, the basal unit of the LMZ, overlies the Giant Mottled Anorthosite of the Bastard Unit (De Klerk, 1995), which is the uppermost unit of the UCZ. Unit N-I is dominated by norite and leuconorite, with the modal proportion of augite only rarely exceeding 10%. The proportion of modal plagioclase is always in excess of 60%, and is usually more than 70%, especially in the central portion of the unit (Fig. 3). Fe-enrichment at the base of the unit is extreme, and inverted pigeonite is a feature of the base of the MZ throughout the Bushveld Complex (von Gruenewaldt and Weber-Diefenbach, 1977; Meyer, 1969; Mitchell, 1990). The inverted pigeonite ($En_{59.4}$ to $En_{60.4}$), together with biotite, is interstitial to plagioclase (Fig. 4a). Apart from the pigeonite in the lowermost 30 m or less of the LMZ, low-Ca pyroxene in the cumulates of Unit N-I occurs as cumulus orthopyroxene grains, usually not more than 2mm in length (Fig. 4b). There is considerable granulation of plagioclase grain boundaries, and of small intercumulus augite grains, throughout the unit. The uppermost sample of unit N-I (A310) displays a pronounced preferred orientation of plagioclase laths and elongate low-Ca pyroxene (Fig. 4c). The cumulates in unit N-I are substantially disrupted in borehole SK2 by transgressive late-stage iron-rich ultramafic pegmatite (IRUP) bodies of various sizes (Fig. 3), detailed descriptions of which are provided by Scoon and Mitchell (1994).

Unit N-II

Unit N-II in the SK2 succession at Union Section is a 102 m thick, leuconorite-dominated sequence containing two feldspathic pyroxenite layers, one (5.5 m thick) at its base, and another (10 m thick) 43.5 m above the base of the unit (Fig. 3). The lower pyroxenite has sharp upper and lower contacts, whilst the uppermost pyroxenite has a sheared upper contact and grades downwards into 0.5 m of mottled anorthosite. The orthopyroxene crystals in the pyroxenites do not have the subrounded, subhedral appearance that typifies cumulus pyroxene in the pyroxenites of the Upper Critical Zone (e.g. Kruger and Marsh, 1985). Rather, they have irregular, sutured outlines (Fig. 5a). Borehole SK4, also at Union Section, contains two pyroxenites at apparently equivalent levels to those in SK2 (Fig. 2), although they are thinner, the lowermost being 5 m thick and the upper 3 m thick. In borehole H5, in the southern sector of the western Bushveld Complex, the two pyroxenite layers, although still present, are reduced to little more than stringers. The basal pyroxenite is 8 cm thick, and there are four stringers, each less than 3 cm thick, within an interval of 1.5 m some 39 m higher up in the succession. The uppermost of the stringers has a sharp upper contact and a gradational lower contact. Unit N-II as a whole is thinner in the H5 succession than at Union Section (Fig. 2). In the interval between the two pyroxenites in the SK2 succession, the leuconorites typically contain poikilitic orthopyroxene grains with rounded inclusions of plagioclase (Fig. 5b), and the rocks do not display the deformation encountered in unit N-I. The leuconorites above the uppermost pyroxenite, on the other hand, are intensely granulated, and orthopyroxene grains contain only small plagioclase inclusions, if any (Fig. 5c).

Unit G-I

Overlying N-II, unit G-I is the first gabbronoritic unit of the LMZ. Unit G-I is clearly delineated on the basis of whole-rock and mineral chemical criteria, and includes in its basal parts the texturally distinctive Porphyritic Gabbronorite (PG). The PG is a conspicuous sequence of rocks that appears between 200 m and 500 m above the base of the LMZ throughout the Bushveld Complex, although it is referred to by different names, e.g. the 'Porphyritic Gabbro Marker' (Mitchell, 1990; Maier and Mitchell 1995), the 'porphyritic cluster norite' (Leeb-Du
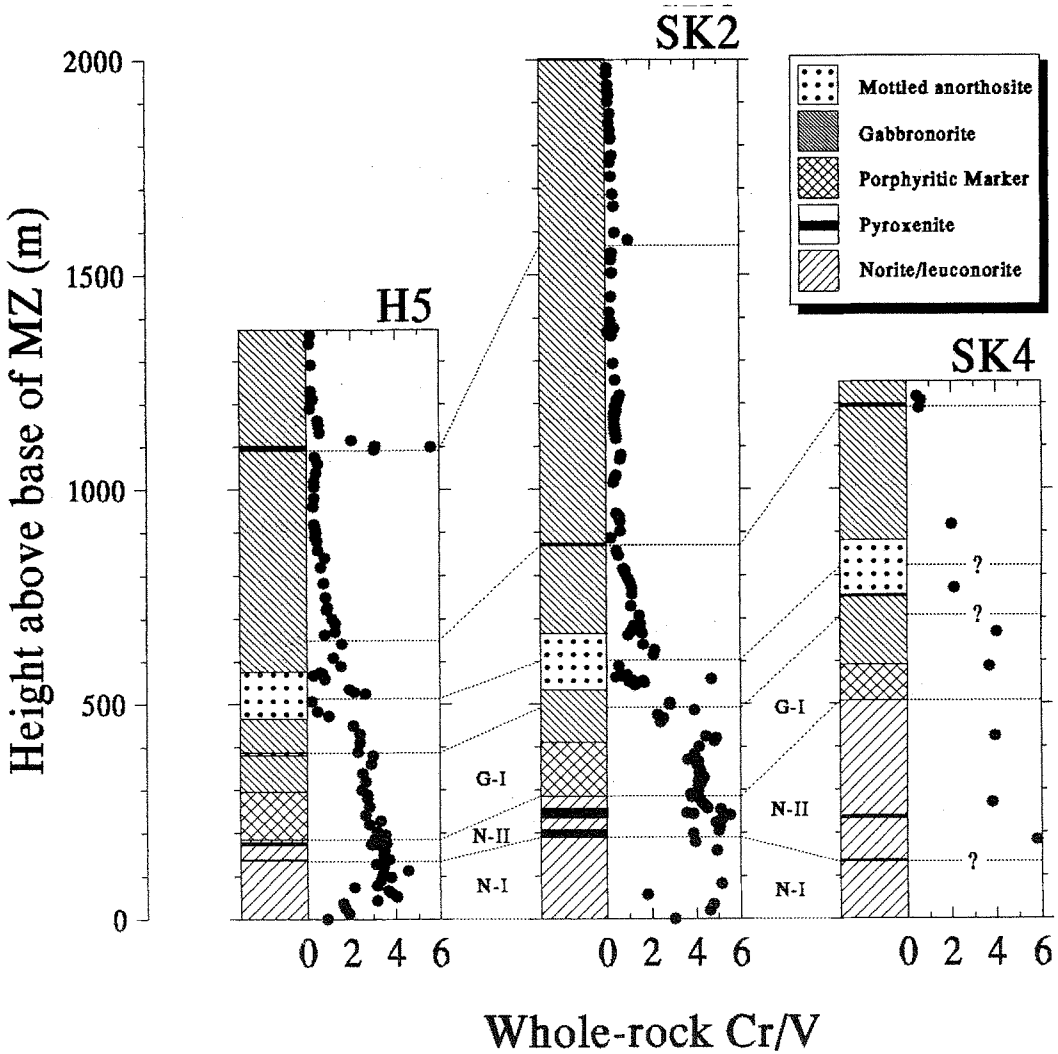
FIG. 2. Stratigraphic correlation between boreholes SK2 and SK4 (RPM Union Section) and borehole H5 (Brits).

Toit, 1986), or the 'porphyritic norite' (Molyneux, 1974; von Gruenewaldt, 1973). Due to its lateral persistence and conspicuous appearance, it is an important marker in exploration drilling for the platiniferous layers of the Upper Critical Zone.

Apart from sample A289, at the base of the unit, the rest of unit G-I contains at least 8.5% modal augite, and usually more than 15% (Fig. 3). The PG, in the basal 110 m of unit G-I, is characterized by a texture in which large (usually up to 5 mm diameter, but sometimes up to 10 mm diameter) orthopyroxene macrocrysts are distrib-

uted throughout a gabbroic matrix in which intercumulus augite crystals seldom exceed 0.5 mm in length (Fig. 6a). The orthopyroxene macrocrysts themselves are poikilitic, enclosing clusters and single crystals of plagioclase. The plagioclase chadacrysts are generally rounded and/or embayed, and range from 1.5 to less than 0.1 mm in length, but many oikocrysts also contain significant numbers of more acicular, euhedral plagioclase chadacrysts up to 1 mm in length (Fig. 6b). There is no systematic distribution of chadacryst sizes within an oikocyst, e.g.
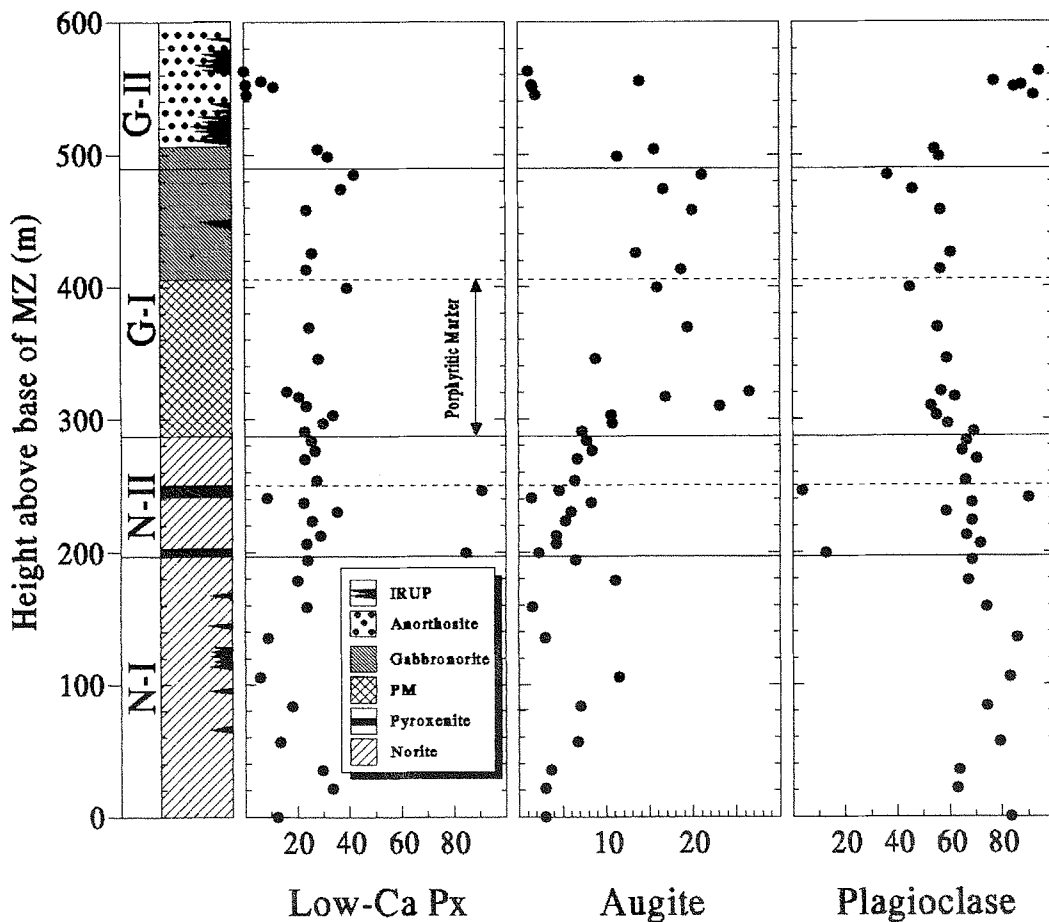
FIG. 3. Generalized stratigraphic column and modal mineralogy of units N-I, N-II and G-I of the Lower Main Zone in borehole SK2.

from small at the centre to large at the margin, as was noted in plagioclase-bearing augite oikocrysts in the Skaergaard intrusion (McBirney and Noyes, 1979). Some orthopyroxene macrocrysts may be essentially cumulus in appearance (Fig. 6a), although most have irregular outlines, indicating adcumulus growth of orthopyroxene in a plagioclase-charged crystal mush (Fig. 6c). In some oikocrysts, certain of the plagioclase chadacrysts may be orientated sub-parallel to a crudely developed mineral layering (Fig. 6b), but this is not always the case. When plagioclase chadacrysts are orientated parallel to lamination in the matrix, it is the acicular grains that reflect the overall fabric of the rock, whilst the the more

rounded or embayed chadacrysts, even within the same oikocryst, display no preferred orientation (Fig. 6b). A directional (linear) fabric is only evident in sections cut perpendicular to the layering. Sections cut in the plane of the layering display no directional orientation, either of the oikocrysts or of their included chadacrysts.

In the SK2 succession, the distinctive brown orthopyroxene macrocrysts of the PG are commonly accentuated by white plagioclase-rich selvages, 1 or 2 mm wide, around their top contacts (Fig. 7). In borehole H5, which is situated in the postulated distal facies of the western Bushveld (Fig. 2), plagioclase selvages are not as well developed around the ortho-
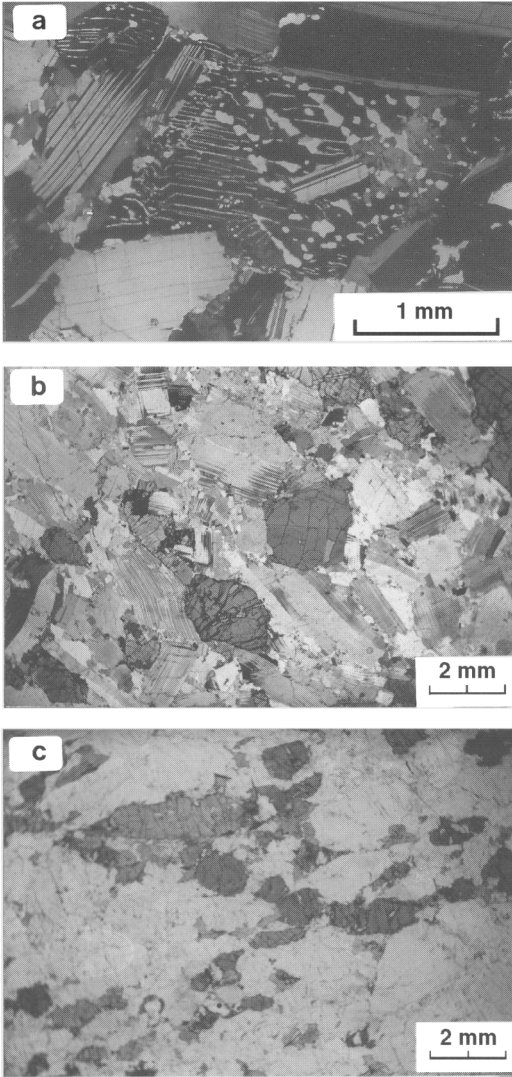
FIG. 4. Photomicrographs of textures in unit N-I of the SK2 succession: (*a*) Intercumulus inverted pigeonite (En$_{59.4}$ to En$_{60.4}$) at the base of unit N-I (sample A343). (*b*) Cumulus orthopyroxene grains in plagioclase matrix. Image enhanced using mica (1/4 λ) plate with crossed polars. Note that plagioclase laths are commonly bent, and have granulated margins (sample A323). (*c*) Sub-parallel orientation of orthopyroxene and plagioclase at the top of unit N-I (sample A310).

FIG. 5. Photomicrographs of textures in unit N-II of the SK2 succession: (*a*) Granulated and sutured boundaries of orthopyroxene grains in the uppermost pyroxenite of unit N-II (sample A297). Similar textures are present in the basal pyroxenite. (*b*) Rounded plagioclase inclusions in orthopyroxene: norite immediately above the basal pyroxenite of unit N-II (sample A308). (*c*) Granulation of plagioclase grain boundaries in norite immediately above the uppermost pyroxenite of unit N-II (sample A295).

pyroxene macrocrysts in the PG. In the latter sequence, the orthopyroxene macrocrysts are accompanied, in places, by large poikilitic grains of intercumulus augite, which contain
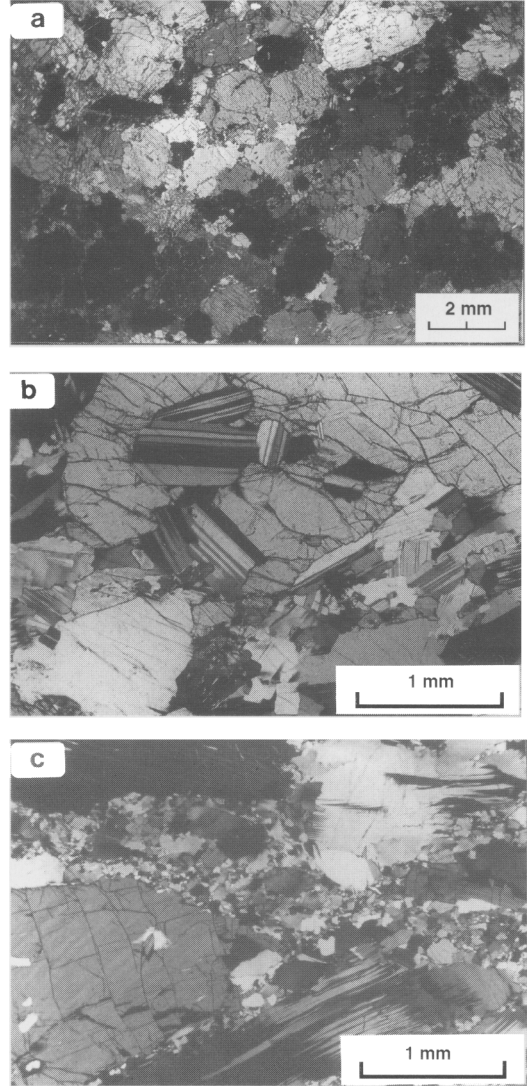
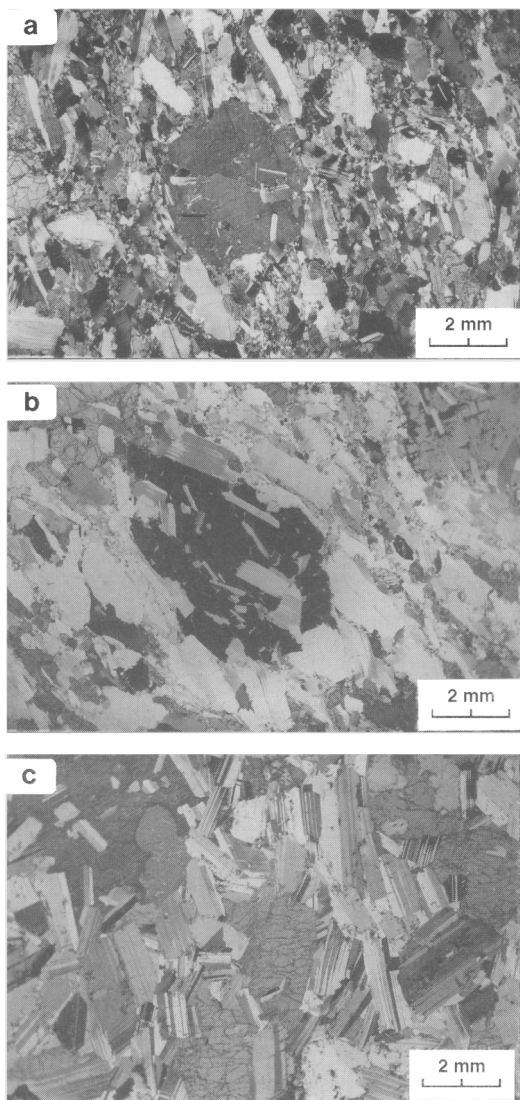chadacrysts of both plagioclase and ortho-pyroxene (Fig. 6*c*).

FIG. 6. Photomicrographs of textures in the Porphyritic Gabbronorite (PG) in the basal part of unit G-I: (a) 30 mm diameter orthopyroxene macrocryst, containing plagioclase inclusions, in a matrix of bent and granulated plagioclase and intercumulus augite. The proportion of intercumulus augite decreases in the immediate vicinity of orthopyroxene macrocrysts. (b) Orthopyroxene macrocryst (black) with crudely sub-parallel plagioclase inclusions in the same orientation as the fabric of the matrix (sample A285). Image enhanced using mica (1/4 λ) plate with crossed polars. (c) Large areas of intercumulus poikilitic augite, enclosing both plagioclase and orthopyroxene, together with poikilitic orthopyroxene macrocrysts, in the PG in borehole H5, in the postulated distal facies of the western Bushveld Complex.

In the upper part of unit G-I, and in the overlying unit G-II, cumulus orthopyroxene crystals are significantly smaller than in the PG (less than 2 mm diameter) and, as a rule, do not contain inclusions of plagioclase. Plagioclase forming the matrix of the rocks is deformed to a greater or lesser extent, deformation twinning and granulated grain margins being common. In some of the more deformed parts of the sequence, there are thin deformation-induced exsolution lamellae of augite along the (100) direction of ortho-pyroxene.

Compositional variations

Analytical procedures

Whole-rock geochemical data (Table 1) were obtained by XRF spectrometry at Rhodes University, Grahamstown and the University of Natal, Pietermaritzburg. Mineral analyses were performed using Cambridge Microscan V and Jeol CXA 733 electron microprobes at Rhodes University, analytical conditions for which are summarized by Mitchell (1990, 1996). Strontium isotope determinations were performed at the Bernard Price Institute, University of the Witwatersrand, using the methods outlined by Kruger (1994).

Unit N-I

There is an up-sequence increase in the Mg# of low-Ca pyroxene through unit N-I in borehole SK2, from 0.609 at the base to 0.720 at the top (Fig. 8a). Although low-Ca pyroxene Mg# data for the cumulates of unit N-I in borehole SK2 are limited, largely due to the presence of a number of transgressive IRUP bodies in this part of the succession, there is an indication that the Mg-enrichment trend may be subdivisible into two or more cycles (Fig. 8a). However, these apparent trends may well be due to postcumulus Fe-enrichment associated with IRUP, as data from borehole H5, which is undisturbed by IRUP, display no similar compositional fluctuations (Fig. 9). Basal Fe-enrichment in unit N-I of the H5 succession is, however, even stronger than in the SK2 succession (Fig. 9). Whole-rock Zr contents are relatively high (17 to 27 ppm) in the Fe-enriched basal 40 m of the unit (Fig. 8b), above which they are lower (10 to 17 ppm). The basal unit of the LMZ in borehole SK2 is characterized by an up-sequence increase in Sr-isotope initial ratios, from 0.70760 at the base to 0.70854 at the

441

TABLE 1. Summarized compositional data for selected samples from units N-I, N-II and G-I of the LMZ

Unit	Sample	Height above base of MZ (m)	Volume % (modal)			Mg#Opx	Whole-rock (ppm)				Sr ^{87}Sr/^{86}Sr$_i$
			Opx	Aug	Plag		Cr	V	Zr	Sr	
G-II	A254	504	28.3	15.6	54.6	—	356	125	7.1	222	0.70841
G-II	A255	499	32.3	11.4	56.1	0.723	355	126	6.1	225	—
G-I	A257	485	42.2	21.1	36.6	0.683	329	84	9.4	177	—
G-I	A260	474	37.0	16.7	46.0	—	412	181	12.3	158	0.70864
G-I	A264	425	25.8	13.5	60.6	0.713	517	117	13.0	251	0.70869
G-I	A266	413	23.8	18.7	56.7	0.722	591	123	7.4	228	—
G-I	A269	399	39.2	16.0	44.8	0.749	440	106	9.4	222	—
G-I	A275	369	24.6	19.5	55.5	0.744	471	130	8.5	228	0.70871
G-I	A280	346	28.1	8.9	59.0	0.740	546	131	7.9	239	—
G-I	A284	321	16.4	26.5	56.9	0.745	559	137	3.6	249	0.70890
G-I	A286	310	23.5	23.2	53.2	0.726	559	137	6.7	222	0.70879
G-I	A287	303	34.0	10.7	55.3	0.735	429	105	15.7	233	0.70889
G-I	A288	297	30.0	10.8	59.3	0.736	517	126	6.9	245	—
G-I	A289	290	23.1	7.3	69.4	0.739	343	91	4.3	275	0.70871
N-II	A290	284	25.6	7.8	66.6	0.714	321	84	3.8	287	—
N-II	A295	254	27.4	6.4	66.0	0.718	438	86	5.1	263	0.70875
N-II	A297	246	90.7	4.6	3.6	0.743	806	224	10.2	16	—
N-II	A299	241	8.6	1.4	90.0	0.746	188	34	2.9	356	0.70842
N-II	A303	223	25.8	5.4	68.6	0.747	443	90	8.1	248	—
N-II	A308	206	23.8	4.3	71.9	0.747	383	76	4.2	271	0.70882
N-II	A309	199	84.7	2.3	12.8	0.744	809	208	8.0	34	0.70865
N-I	A310	194	24.1	6.5	68.6	0.720	—	—	—	—	—
N-I	A312	179	20.2	11.1	67.1	0.713	335	84	16.2	275	0.70854
N-I	A315	159	23.8	1.6	74.3	—	372	75	11.3	284	0.70843
N-I	A327	83	18.0	7.1	74.4	0.732	345	67	11.3	306	0.70800
N-I	A340	21	33.5	3.0	63.0	—	419	91	18.6	280	0.70780
N-I	A343	0	12.5	3.0	83.5	0.609	191	63	17.8	332	0.70760

Mg#Opx = atomic ratio Mg/(Mg+Fe)
^{87}Sr/^{86}Sr$_i$ = initial ratio (2060 my)

top of the unit (Fig. 8b). This latter trend is not developed in the H5 succession (Fig. 9).

Unit N-II

The most obvious compositional change at the base of unit N-II in SK2 is the increase in the low-Ca pyroxene Mg#, from a mean of 0.720 in the uppermost sample of unit N-I to 0.744 in the basal pyroxenite of unit N-II (Fig. 8a). The Mg# is restricted within the range 0.735 to 0.750 in the basal 50 m of unit N-II (i.e. including the basal and upper pyroxenites and the intervening norite). In the upper portion of unit N-II (above the upper pyroxenite), the Mg# of low-Ca pyroxene is significantly lower, ranging between 0.721 and

0.708. The separation of the lower and upper parts of unit N-II in terms of low-Ca pyroxene Mg# is less clearly defined in the H5 succession than in SK2 (Fig. 9).

The Sr isotope initial ratio is 0.70865 in the basal pyroxenite of unit N-II in SK2, but increases to 0.70882 in a norite sample 7 m above the pyroxenite (Fig. 8b). The initial ratio is slightly lower (0.70842) in the anorthosite immediately below the upper pyroxenite, and is 0.70875 in the norite above the upper pyroxenite. The whole-rock Zr content of unit N-II is lower than that of unit N-I (8 ppm or less in the norites, and up to 10 ppm in the upper pyroxenite). Apart from the pyroxenite layers, there is no distinctive pattern to Zr concentrations in unit N-II (Fig. 8b).
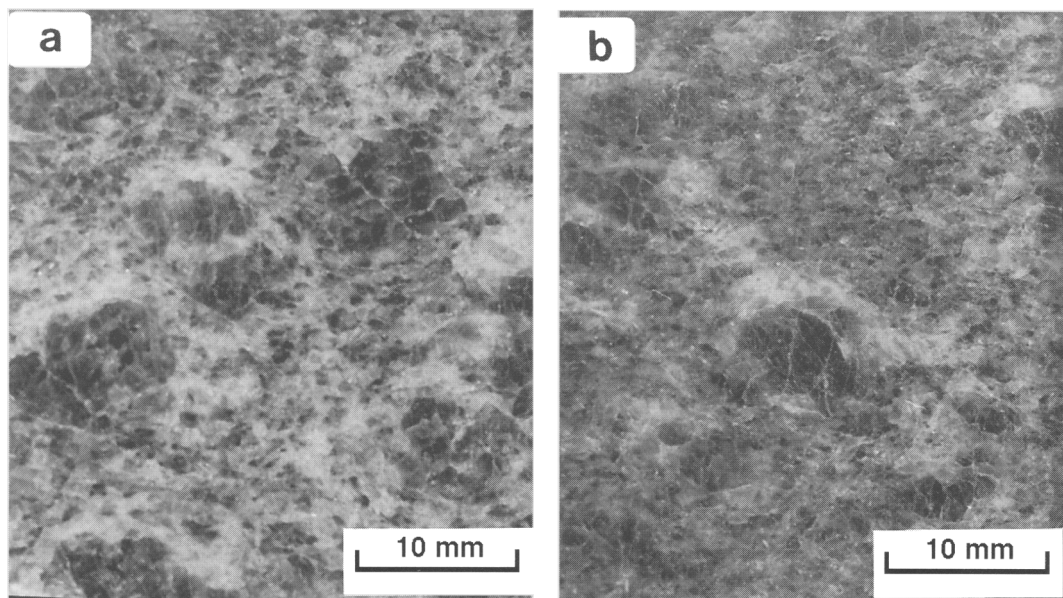
FIG. 7. The Porphyritic Gabbronorite in hand specimen, showing distinctive orthopyroxene macrocrysts, with plagioclase-rich selvages around their upper margins, in a gabbroic matrix. (*a*) Sample A278, 334 m above base of Main Zone. (*b*) Sample A281, 341 m above base of Main Zone.

Unit G-I

There is an abrupt increase in low-Ca pyroxene Mg#, from a mean of 0.714 in sample A290, at the top of unit N-II, to 0.739 in sample A289, at the base of unit G-I. Although regarded as the base of the unit on the basis of the low-Ca pyroxene Mg#, sample A289 still displays the petrographic characteristics of the underlying units N-I and N-II, with which it shares many chemical similarities, including whole-rock Cr, V and Sr contents and the Sr isotope initial ratio (Figs. 8*a*, 9). It is only in sample A288, 7 metres above the base of the unit, that the true characteristics of unit G-I begin to manifest themselves. These include an increase in the modal proportion of augite, accompanied by the development of the distinctive texture of the Porphyritic Gabbronorite, as well as increases in whole-rock Cr and V contents. It is also notice-able that the Sr isotope initial ratio is higher (0.70889) in sample A287, 13 m above the base of the unit, than in sample A289 (0.70871) at the base of the unit. Throughout the PG, the Mg# of orthopyroxene ranges from a low of 0.725 to a high of 0.752.

There is a sharp decrease in orthopyroxene Mg#, from a mean of 0.749 in sample A269 at the top of the PG, to 0.722 in sample A266, in the upper part of unit G-I. In contrast to the PG, where the orthopyroxene Mg# remains relatively constant throughout, the upper part of unit G-I displays a trend of decreasing Mg#, from a mean of 0.722 in sample A266 to 0.683 in sample A257, near the top of the unit. Although sample A266, immediately above the PG, has a relatively low Zr content, the remainder of the upper part of unit G-I has a higher Zr content than does the PG.

As is the case in the underlying units, compositional variation is more muted in unit G-I of the H5 succession than in the SK2 succession.

Summary of significant data

Unit N-I, at the base of the Main Zone, is almost exclusively leuconoritic. The base of the unit displays significant iron-enrichment, manifested primarily in the presence of intercumulus inverted pigeonite, as opposed to cumulus orthopyroxene in the remainder of the unit. The Fe-enriched
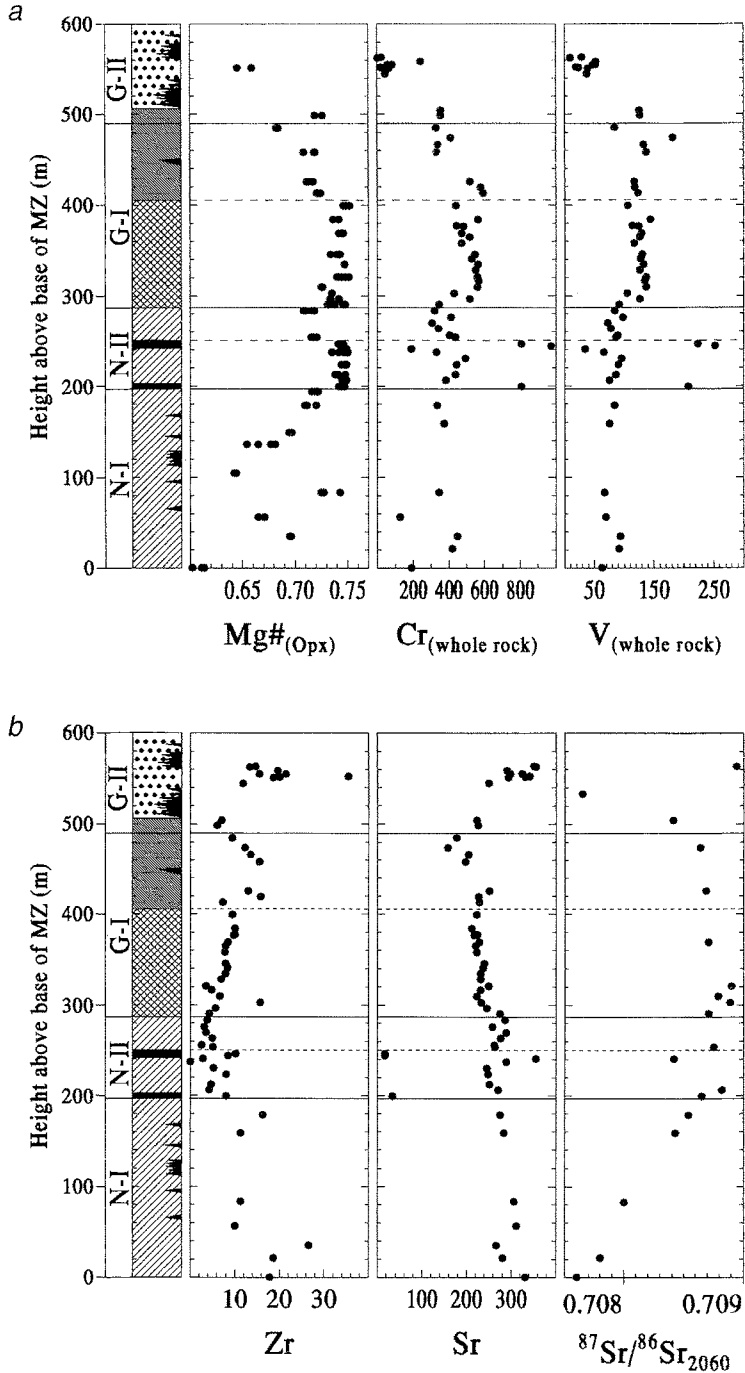
FIG. 8(*a*). Stratigraphic variations in Mg# [atomic ratio Mg/(Mg+Fe)] of low-Ca pyroxene, whole-rock Cr, and whole-rock V, in units N-I, N-II and G-I of the Lower Main Zone in borehole SK2 (RPM Union Section). (*b*) Stratigraphic variations in whole-rock Zr and Sr, and the whole-rock $^{87}Sr/^{86}Sr$ isotope initial ratio, in units N-I, N-II and G-I of the Lower Main Zone in borehole SK2 (RPM Union Section).
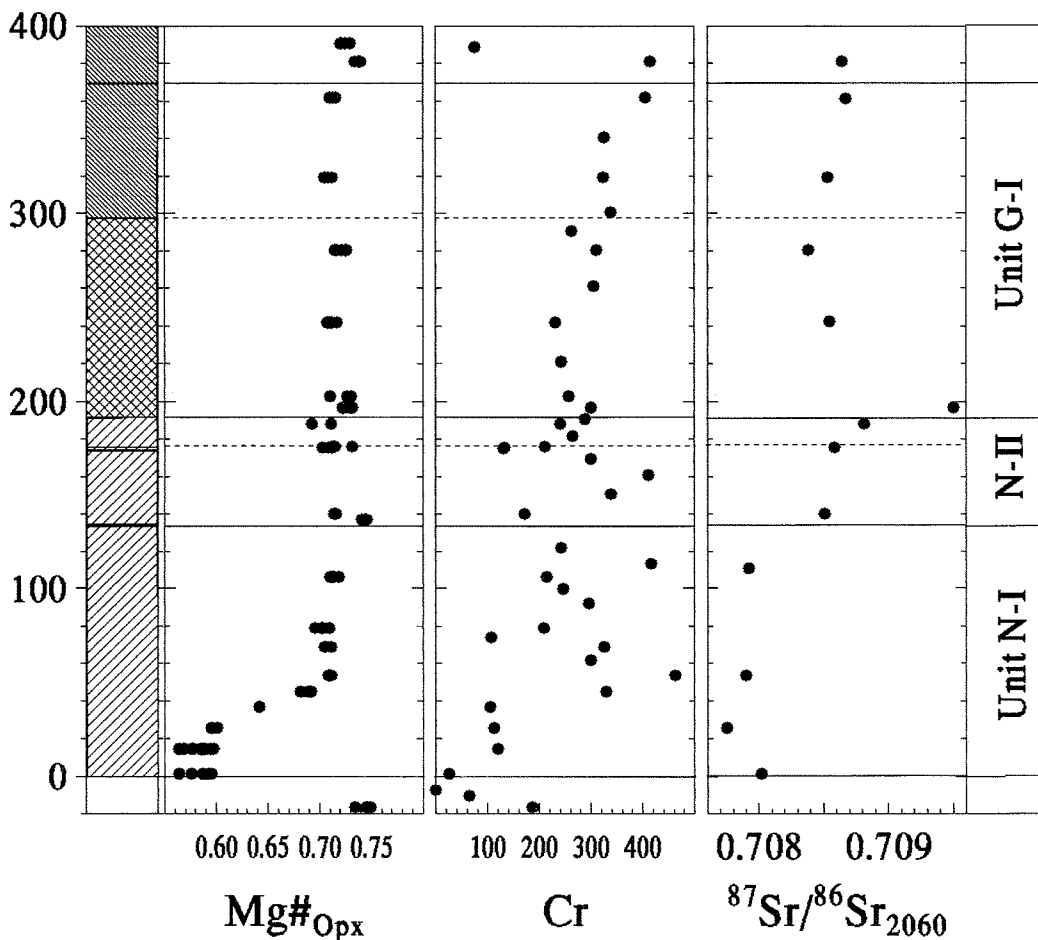
FIG. 9. Stratigraphic variations in Mg# [atomic ratio Mg/(Mg+Fe)] of low-Ca pyroxene, whole-rock Cr, and the whole-rock $^{87}Sr/^{86}Sr$ isotope initial ratio, in units N-I, N-II and G-I of the Lower Main Zone in borehole H5 (Brits district).

basal part of N-I also displays relatively high whole-rock Zr contents. There is a progressive increase in the Sr isotope initial ratio upwards through the unit in the SK2 succession, but this trend is not developed in borehole H5. Complex patterns of variation in the low-Ca pyroxene Mg# of this unit in the SK2 succession may be due in part to processes related to those by which the numerous bodies of discordant IRUP in the unit formed. There are no Mg# fluctuations in the H5 succession, but basal Fe-enrichment at the base of unit N-I is more extreme in H5 than in SK2.

Units N-II and G-I, similar to one another in many respects, but differing in significant details, are the primary focus of this paper. The most

obvious difference between the two is that unit N-II is predominantly noritic, apart from two orthopyroxenite layers, whilst unit G-I is the first of the substantially gabbronoritic units in the Main Zone. On the other hand, both units are characterized by elevated Sr isotope initial ratios, amongst the highest in the whole Bushveld layered succession, particularly at their bases.

Orthopyroxene Mg# data display similar patterns in N-II and G-I, the lower part of each unit having an elevated and remarkably constant Mg# over a significant stratigraphic interval (of the order of 46 m in N-II, and close to 110 m in G-I). In the upper part of each unit, there is a sharp inflection to lower Mg#, followed by a

further progressive decline to the top of the unit. The interval of high Mg# in unit N-II is bounded top and bottom by orthopyroxenite layers, whilst in unit G-I the interval of elevated Mg# corresponds to the distinctive Porphyritic Gabbronorite. In both units, the relatively Mg-rich orthopyroxene in the basal interval is poikilitic, containing significant numbers of rounded and embayed or acicular plagioclase inclusions.

Whole-rock Zr contents are low in unit N-II, and in the PG at the base of unit G-I, suggesting an absence of residual, fractionated material. The Zr content of the cumulates between the pyroxenites in unit N-II is, however, generally slightly higher than in the uppermost part of the unit (Fig. 8b). It is perhaps also significant that unit N-II and the overlying Porphyritic Gabbronorite (the lower part of unit G-I) are the only parts of the LMZ succession in borehole SK2 that are unaffected by IRUP, which are characteristically developed in highly fractionated plagioclase-rich cumulates (Scoon and Mitchell, 1994).

Discussion

Unit N-I

In the proximal SK2 succession, unit N-I of the LMZ displays a systematic up-sequence increase in the Sr isotope initial ratio that marks it as transitional between the UCZ magmatic lineage below the Merensky Reef and the typically MZ lineage of units N-II and above. At its base, it displays the most substantial Fe-enrichment to be found anywhere below the Upper Zone, other than in transgressive IRUP bodies.

The combination of increasing orthopyroxene Mg# and increasing Sr isotope initial ratios upward through unit N-I has been ascribed to progressive influx, mixing, and crystallization of small batches of new, Main Zone-type magma with the resident residual magma in the chamber (Eales *et al.*, 1986; Mitchell, 1990). Even if magma mixing were the main process involved, however, the Fe-enrichment at the base of the unit is too substantial to be the result simply of fractionation from a hybrid magma. Postcumulus downward draining of late-stage Fe-rich intercumulus liquids (Mitchell, 1990; Scoon and Mitchell, 1994), with consequent subsolidus Fe-enrichment of pyroxenes due to trapped liquid shift (Barnes, 1986), provides a mechanism for the observed compositional trends. Further support for the trapped liquid shift hypothesis is

the relative enrichment in Zr at the base of the unit. In contrast to the proximal (SK2) succession, the distal (H5) lithologies of unit N-I do not display an upward increase in Sr isotope initial ratio. This suggests that the new magma influxes may not initially have spread as far as the distal parts of the Complex.

Unit N-II

In the three boreholes investigated, the basal portion of unit N-II is bounded by pyroxenite layers. Ultramafic layers within plagioclase-rich cumulate sequences are commonly interpreted as the products of fresh injections of magma (Scoon and De Klerk, 1987; Campbell and Turner, 1989; Mitchell, 1996). It would therefore be reasonable to assume, as a starting hypothesis, that the two pyroxenite layers in unit N-II are the basal layers of two successive cyclic units, similar in essence to the Merensky and Bastard units at the top of the Upper Critical Zone. In contrast to typical cyclic units, however, there is no evidence of any substantial fractionation in the plagioclase-rich cumulates overlying the basal pyroxenite of the unit. Indeed, orthopyroxene from many samples of the noritic cumulates between the pyroxenites has higher Mg# values than either the basal or the upper pyroxenite. The noritic cumulates between the pyroxenites are also distinguished, especially from those in the upper part of the unit, by the fact that they are poikilitic, containing plagioclase chadacrysts. The presence of plagioclase-bearing pyroxene oikocrysts in cumulates has been related to entrainment of plagioclase from evolved resident liquid by magma freshly injected into the chamber (Eales *et al.*, 1991; Maier and Eales, 1994b), or to constitutional supercooling of fresh influxes of magma (Mathison, 1987; Tegner and Wilson, 1995; Krynauw and Wilson, 1995). Regardless of whether the oikocrysts are due to entrainment of allochthonous plagioclase or to supercooling, both textural and compositional evidence would seem to support a model whereby the poikilitic norites between the pyroxenites in N-II, as well as the pyroxenites themselves, are the products of a single injection of magma.

Hill *et al.* (1995) suggested that cumulate layers in thick komatiite flows develop when high magma flow rates result in continuous replenishment of fresh solute at the site of crystallization. It was suggested by Mitchell (1996) that at least some adcumulate pyroxenites in layered intru-

sions may similarly develop in regimes of high magma flow rate. Following this reasoning, the two pyroxenites may be the adcumulate top and bottom contact manifestations of a single magma injection, separated by orthocumulates that represent stagnating conditions in the same event. This implies separate origins for the cumulates of the lower and upper parts of unit N-II, those between the pyroxenites representing the crystallization products of fresh magma, whilst those in the upper part of the unit represent evolved resident liquid, beneath which the new magma was injected with minimal intermixing.

Unit G-I and the Porphyritic Gabbro

In the lowermost 110 m of unit G-I in borehole SK2, large orthopyroxene oikocrysts (5 to 10 mm diameter), set in a finer-grained gabbroic matrix, impart the distinctive porphyritic texture of the PG. Poikilitic cumulates, in which pyroxene or olivine oikocrysts enclose plagioclase chadacrysts, have been described from several different intrusions (Wager and Brown, 1968; Cameron, 1969; McBirney and Noyes, 1979; Mathison, 1987; Eales et al., 1990a,b, 1991; Wilson, 1992; Maier and Eales, 1994b; Maier, 1995; Tegner and Wilson, 1995; Krynauw and Wilson, 1995; McBirney and Hunter, 1995). A comprehensive criticism of classical cumulate terminology by McBirney and Hunter (1995), in which the interpretation of poikilitic cumulates features prominently, is a contemporary reflection of doubts about the adequacy of the cumulate terminology that have arisen periodically over the past 25 years or more, often prompted specifically by poikilitic textures (Cameron, 1969; Campbell, 1978; Mathison, 1987).

Most commonly, the discussion of poikilitic cumulates refers to clinopyroxene (augite) oikocrysts enclosing plagioclase chadacrysts (Mathison, 1987; Tegner and Wilson, 1995), although olivine oikocrysts are also present in several intrusions (Mathison, 1987; Maier, 1995), as are orthopyroxene oikocrysts (Maier and Eales, 1994b). Poikilitic cumulates are commonly located at or near the base of demonstrable cyclic units, and various features of the rocks, including the small size of plagioclase chadacrysts relative to matrix plagioclase, and their high degree of mutual attachment, are cited as evidence for supercooling of the order of 20 to 45 °C (Mathison, 1987; Tegner and Wilson, 1995; Krynauw and Wilson, 1995). The spatial distribu-

tion of plagioclase chadacrysts has been used as an indication that the pyroxene oikocrysts crystallized within a plagioclase crystal mush containing of the order of 50% crystals (Mathison, 1987; Tegner and Wilson, 1995). The presence of both euhedral and embayed or rounded chadacrysts in some pyroxene oikocrysts (Mathison, 1987; Tegner and Wilson, 1995) has been regarded as something of a conundrum, especially as there is no reaction relationship between pyroxene or olivine and plagioclase that might explain the resorption features (Mathison, 1987). Tegner and Wilson (1985) suggested that most of the partially resorbed chadacrysts crystallized from residual resident liquid in the chamber prior to magma addition, whilst the remaining chadacrysts, specifically the more euhedral examples, crystallized from new and/or mixed magma. Tegner and Wilson (op. cit.) also noted a closer grain centre spacing amongst chadacrysts than amongst matrix plagioclase grains, and attributed this to sub-solidus textural equilibration of matrix grains during compaction.

In most of the cases described, the mafic oikocrysts are large (5 to 20 mm diameter), are unquestionably intercumulus in appearance, and are almost always olivine or augite, but rarely orthopyroxene. The oikocrysts described here from the PG, by contrast, are almost invariably orthopyroxene, except in isolated cases in the distal H5 sequence, and are commonly cumulus in appearance, in that they appear to have crystallized prior to most of the matrix plagioclase. They are also significantly smaller than the augite oikocrysts described by e.g. Mathison (1987), Tegner and Wilson (1995) and Krynauw and Wilson (1995).

Mathison (1987) suggested that plagioclase chadacrysts might well be the remains of self-nucleated clusters resulting from supercooling in situ, followed by crystallization of the oikocrysts, also mostly in situ. It is primarily this assumption of in situ crystallization of both plagioclase and orthopyroxene, under conditions that were by implication relatively stagnant, that makes the interpretation of coexisting euhedral and resorbed chadacrysts in the same pyroxene oikocryst difficult. These problems are overcome if crystallization is assumed to have occurred, at least partially, in a dynamic magma flow regime. The work of Eales et al. (1988, 1990a, 1991, 1994) and Scoon and Teigler (1995) has demonstrated the validity of facies models for the Upper Critical Zone of the western Bushveld Complex. It is

becoming evident that the layered sequence of the Lower Main Zone, although not as dramatically developed as that of the Upper Critical Zone, is nevertheless equally persistent laterally. The validity of the facies model relies on lateral movement of magma along strike from the locus of injection. If the fresh magma was intruded into a plagioclase crystal-rich mush, it would have scavenged a truly allochthonous assemblage of grains as it spread laterally. The degree of resorption of plagioclase chadacrysts, although controlled partially by composition, would also be an indication of residence time in the magma. Highly rounded chadacrysts would therefore be assumed to have been entrained and carried some distance from their site of crystallization, whilst more euhedral grains would have had a relatively shorter residence time in the magma. Finally, euhedral chadacrysts *in the the same orientation* as a preferred orientation in the matrix of the rock could be interpreted as having crystallized *in situ*.

The plagioclase-rich selvages around the top contacts of orthopyroxene macrocrysts in the SK2 succession (Fig. 7) are attributed to the rise of low-density rejected solute, rich in plagioclase components, as a result of crystallization and growth of the orthopyroxene grains. It is perhaps significant that in the distal facies, where relatively rapid cooling would have curtailed the rise of the rejected solute, this texture is not as well developed.

Conclusions

Unit N-I, at the base of the LMZ, displays an up-sequence increase in the Sr isotope initial ratio in the proximal facies, indicating progressive hybridization of resident liquid with periodic small influxes of new magma. The absence of this pattern from the distal facies indicates that these small influxes only penetrated a limited distance into the magma chamber. Fe-enrichment, manifested in intercumulus pigeonite, together with enhanced whole-rock Zr concentrations, indicate downward migration of highly evolved postcumulus liquid, with attendant trapped liquid shift, at the base of unit N-I.

Units N-II and G-I, overlying unit N-I, both represent significant injections of new magma into the magma chamber. Whole-rock Sr isotope initial ratios are very high (close to 0.709 in SK2, and in excess of 0.709 in H5) near the base of both units, indicating the first major injections of truly LMZ-type magma. The lower part of each

unit has uniformly high orthopyroxene Mg#, indicating that replenishment processes dominated, with little or no fractionation. In each of the two units, the sharp discontinuity between a relatively primitive basal sequence and an evolved upper sequence suggests very little magma mixing betweeen the new magma at the base and the fractionated resident material above. This may be ascribed to a density contrast between two liquid layers. Alternatively it may be the result of sill-like injection of new magma into an already substantially crystalline mush, along the lines suggested by Lee and Butcher (1990) and Mitchell (1996) for other parts of the Bushveld layered succession.

In the case of unit N-II, the presence of upper and lower pyroxenite layers indicates fairly rapid nucleation and growth of orthopyroxene under conditions of high flow rate. By contrast, the orthocumulate textures, allied to the relative absence of fractionation, in the noritic cumulates between the pyroxenites indicates relatively less dynamic conditions of crystallization.

Poikilitic, plagioclase-bearing orthopyroxene grains, which are spectacularly developed in unit G-I but which also occur in unit N-II, are not related to supercooling and *in situ* crystallization (Mathison, 1987; Tegner and Wilson, 1995; Krynauw and Wilson, 1995) Rather, they represent entrainment of pre-existing plagioclase grains by laterally flowing magma injected into a crystal-charged mush. The rounded shapes of the plagioclase inclusions, and the embayments in many, are difficult to account for by any process other than resorption. Such shapes are wholly atypical of plagioclase feldspar that has grown as a primocrystal or intercumulus phase.

In a study of plagioclase grain-size distributions in the Main Zone, Maier and Mitchell (1995) showed that there is a progressive upward increase in plagioclase grain-size in each of units N-I, N-II and G-I. The grain size increase towards the top of each unit may indicate annealing as a response to reheating by intruding magma of the succeeding unit. If this postulate is correct, it strengthens the multiple intrusion hypothesis advanced here.

Acknowledgements

References

Barnes, S.J. (1986) The effect of trapped liquid crystallization on cumulus compositions in layered intrusions. *Contrib. Mineral. Petrol.*, **93**, 524–31.

Cameron, E.N. (1969) Postcumulus changes in the eastern Bushveld Complex. *Amer. Mineral.*, **54**, 754–79.

Campbell, I.H. (1978) Some problems with the cumulus theory. *Lithos*, **11**, 311–23.

Campbell, I.H. and Turner, J.S. (1989) Fountains in magma chambers. *J. Petrol.*, **30**, 885–923.

Cawthorn, R.G., Meyer, P.S. and Kruger, F.J. (1991) Major addition of magma at the Pyroxenite Marker in the western Bushveld Complex, South Africa. *J. Petrol.*, **32**, 739–63.

De Klerk, W.J. (1995) Textures exhibited by feldspars in the Giant Mottled Anorthosite (GMA) of the Bastard Unit in the Upper Critical Zone, Western Bushveld Complex. *Mineral. Petrol.*, **54**, 25–34.

Eales, H.V., Field, M., de Klerk, W.J. and Scoon, R.N. (1988) Regional trends of chemical variation and thermal erosion in the Upper Critical Zone, western Bushveld Complex. *Mineral. Mag.*, **52**, 63–79.

Eales, H.V., Marsh, J.S., Mitchell, A.A., De Klerk, W.J., Kruger, F.J. and Field, M. (1986) Some geochemical constraints upon models for the crystallization of the Upper Critical Zone-Main Zone interval, northwestern Bushveld Complex. *Mineral. Mag.*, **50**, 567–82.

Eales, H.V., De Klerk, W.J., Butcher, A.R. and Kruger, F.J. (1990a) The cyclic unit beneath the UG1 chromitite at RPM Union Section platinum mine. *Mineral. Mag.*, **54**, 23–43.

Eales, H.V., De Klerk, W.J. and Teigler, B. (1990b) Evidence for magma mixing processes within the Critical and Lower Zones of the northwestern Bushveld Complex. *Chem. Geol.*, **88**, 261–78.

Eales, H.V., Maier, W.D. and Teigler, B. (1991) Corroded plagioclase inclusions in orthopyroxene and olivine in the Lower and Critical Zones, Western Bushveld Complex. *Mineral. Mag.*, **55**, 479–86.

Eales, H.V., De Klerk, W.J. Teigler, B. and Maier, W.D. (1994) Nature and origin of orthopyroxenites in the western Bushveld Complex, in the light of compositional data. *S. Afr. J. Geol.*, **97**, 399–407.

Hamilton, J (1977) Sr isotope and trace element studies of the Great Dyke and Bushveld mafic phase and their relationship to early magma genesis in southern Africa. *J. Petrol.*, **18**, 24–52.

Hill, R.E.T., Barnes, S.J., Gole, M.J. and Dowling, S.E. (1995) The volcanology of komatiite as deduced from field relationships in the Norseman-Wiluna greenstone belt, Western Australia. *Lithos*, **34**, 159–88.

Kruger, F.J. (1994) The Sr-isotopic stratigraphy of the western Bushveld Complex. *S. Afr. J. Geol.*, **97**, 393–98.

Kruger, F.J. and Marsh, J.S. (1982) The significance of $^{87}Sr/^{86}Sr$ ratios in the Merensky cyclic unit of the Bushveld Complex. *Nature*, **298**, 53–5.

Kruger, F.J. and Marsh, J.S. (1985) The mineralogy, petrology, and origin of the Merensky Cyclic Unit in the western Bushveld Complex. *Econ. Geol.*, **80**, 958–74.

Krynauw, J.R. and Wilson, A.H. (1995) Evidence for constitutional supercooling from orthopyroxene-pigeonite-plagioclase relations in the Borgmassivet suite of western Dronning Maud Land, Antarctica. *Mineral. Petrol.*, **54**, 119–36.

Lee, C.A. and Butcher, A.R. (1990) Cyclicity in the Sr isotope stratigraphy through the Merensky and Bastard Reef units, Atok Section, eastern Bushveld Complex. *Econ. Geol.*, **85**, 877–83.

Leeb-Du Toit, A. (1986) The Impala Platinum Mines. In *Mineral Deposits of Southern Africa*, II. (C.R. Anhaeusser and S. Maske, eds.). Geol. Soc. S. Afr., 1091–106.

Maier, W.D. (1995) Olivine oikocrysts in Bushveld anorthosite: some implications for cumulate formation. *Canad. Mineral.*, **33**, 1011–22.

Maier, W.D. and Eales, H.V. (1994a) Facies model for the interval bwtween UG2 and Merensky Reef, western Bushveld Comlex, South Africa. *Trans. Inst. Mining Metall.*, **103**, B1–B86.

Maier, W.D. and Eales, H.V. (1994b) Plagioclase inclusions in orthopyroxene and olivine of the UG2-Merensky Reef interval: regional trends in the western Bushveld Complex. *S. Afr. J. Geol.*, **97**, 408–14.

Maier, W.D. and Mitchell, A.A. (1995) Grain size variations of cumulus plagioclase in the Main Zone of the Bushveld Complex. *Eur. J. Mineral.*, **7**, 195–204.

Mathison, C.I. (1987) Pyroxene oikocrysts in troctolitic cumulates – evidence for supercooled crystallization and postcumulus modification. *Contrib. Mineral. Petrol.*, **97**, 228–36.

McBirney, A.R. and Hunter, R.H. (1995) The cumulate paradigm reconsidered. *J. Geol.*, **103**, 114–22.

McBirney, A.R. and Noyes, R.M. (1979) Crystallization and layering in the Skaergaard Intrusion, East Greenland: preliminary observations. *J. Petrol.*, **20**, 487–554.

Meyer, C. (1969) *Some petrological aspects of mafic rocks from four borehole sections between the Merensky Reef and the Main Zone gabbro in the western and eastern Bushveld Complex.* Unpubl. M.Sc. thesis, Potchefstroom Univ., 91 p.

Mitchell, A.A. (1990) The stratigraphy, petrography and mineralogy of the Main Zone of the northwestern Bushveld Complex. *S. Afr. J. Geol.*, **93**, 818−31.

Mitchell, A.A. (1996) Compositional cyclicity in a pyroxenitic layer from the Main Zone of the Western Bushveld Complex: evidence for repeated magma influx. *Mineral. Mag.*, **60**, 149−61.

Molyneux, T.G. (1974) A geological investigation of the Bushveld Complex in Sekhukhuneland and part of the Steelpoort valley. *Trans. Geol. Soc. S. Afr.*, **77**, 329−38.

Scoon, R.N. and De Klerk, W.J. (1987) The relationship of olivine cumulates and mineralization to cyclic units in part of the Upper Critical Zone of the western Bushveld Complex. *Canad. Mineral.*, **25**, 51−77.

Scoon, R.N. and Mitchell, A.A. (1994) Discordant iron-rich ultramafic pegmatites in the Bushveld Complex and their relationship to iron-rich intercumulus and residual liquids. *J. Petrol.*, **35**, 881−917.

Scoon, R.N. and Teigler, B. (1994) Platinum-group element mineralization in the Critical Zone of the western Bushveld Complex: I. Sulfide-poor chromitites below the UG-2. *Econ. Geol.*, **89**, 1094−121.

Sharpe, M.R. (1985) Strontium isotope evidence for preserved density stratification in the main zone of the Bushveld Complex, South Africa. *Nature*, **316**, 119−26.

Tegner, C. and Wilson, J.R. (1995) Textures in a poikilitic olivine gabbro cumulate: evidence for supercooling. *Mineral. Petrol.*, **54**, 161−73.

von Gruenewaldt, G. (1973) The Main and Upper Zones of the Bushveld Complex in the Roossenekal area, eastern Transvaal. *Trans. Geol. Soc. S. Afr.*, **76**, 207−27.

von Gruenewaldt, G. and Weber-Diefenbach, K. (1977) Coexisting Ca-poor pyroxenes in the Main Zone of the Bushveld Complex. *Contrib. Mineral. Petrol.*, **65**, 11−18.

Wager, L.R. and Brown, G.M. (1968) *Layered Igneous Rocks.* Oliver & Boyd, Edinburgh, 588 pp.

Wilson, A.H. (1992) The geology of the Great Dyke, Zimbabwe: crystallization, layering and cumulate formation in the P1 Pyroxenite of Cyclic unit 1 of the Darwendale Subchamber. *J. Petrol.*, **33**, 611−63.